22 Tunneling Current of the Contact of the Curved Graphene Nanoribbon with Metal and Quantum Dots

Mikhail B. Belonenko, Natalia N. Konobeeva,
Alexander V. Zhukov, and Roland Bouffanais

CONTENTS

ABSTRACT

In this chapter, we present the overview of our recent studies on the electron spectrum and the density of states of long-wave electrons in curved graphene nanoribbons, based on the Dirac equation in a curved space–time. The current–voltage characteristics for the contact of nanoribbon–quantum dots and nanoribbon–metal have been revealed. The dependence of the specimen properties on its geometry was analyzed. Also the regions with negative differential conductivity were found.

22.1 INTRODUCTION

Few decades ago, it has been well realized that the gauge invariance plays a key role in the quantum field theory (QFT) description of fundamental interactions between elementary particles. The recent comprehensive review by Vozmediano et al. [1] presents a detailed picture of the relation between QFT and the condensed matter physics of graphene. In this chapter, we only briefly overview certain key points before going directly to the matter of our study.

The mathematical concept of a non-Abelian gauge field introduced first in QFT for a description of the electroweak interaction, followed by the experimental discovery of the W and Z bosons, is an example of the most impressive achievements of theoretical physics. Before introducing the various gauge fields associated with the physics of graphene and in order to clarify their specific nature, we will make a brief description of the classical concept of gauge invariance and of the associated gauge fields [1].

The concept of gauge invariance has been naturally introduced in classical electrodynamics. In particular, the electromagnetic field ($\mathbf{E}$, $\mathbf{B}$) is expressed in terms of the potentials (Φ, $\mathbf{A}$) through

$$E = -(\nabla\Phi + \partial_t \mathbf{A}), \quad \mathbf{B} = \nabla \times \mathbf{A}. \tag{22.1}$$

The fields do not change under the transformation

$$\mathbf{A} \rightarrow \mathbf{A} + \nabla\chi, \quad \Phi \rightarrow \Phi - \partial t \chi, \tag{22.2}$$

where χ is an arbitrary scalar function of coordinate. This invariance was shown to remain applicable to the quantum mechanics of a charged spinless particle in an electromagnetic field provided that the wave function was simultaneously transformed as

$$\Psi \rightarrow \Psi\exp(ie\chi). \tag{22.3}$$

The relativistic wave equation for a spinless particle with charge e interacting with electromagnetic fields is derived by first performing the substitution $p_\mu \rightarrow p_\mu - eA_\mu$, where $A_\mu = (A^0 = \Phi, A)$ is the 4-vector electromagnetic potential, and then performing the usual substitution $p_\mu \rightarrow i\hbar\partial_\mu$. A formal solution for the wave function of a particle interacting with

327

the electromagnetic potential A_μ can be written in terms of the solution without interaction

$$\psi = \exp\left[-ie\int A^\mu dx_\mu\right]\psi_0. \tag{22.4}$$

Quantum dynamics, that is, the form of the quantum equation, remains unchanged by the transformations (22.2) if the wave function of the particle is multiplied by a local (space–time-dependent) phase.

The first example of a QFT gauge model is four-dimensional quantum electrodynamics (QED). A free spin 1/2 Dirac fermion with charge e and mass m is described by the action integral

$$S_\psi = \int d^4x\,\overline{\psi}[\gamma^\mu\partial_\mu + m]\psi, \tag{22.5}$$

which is invariant under the global $U(1)$ group of transformations:

$$\psi(x) \to U\psi(x), \quad \overline{\psi}(x) \to U^*\overline{\psi}(x), \quad U = \exp(ie\chi), \tag{22.6}$$

where χ is a constant. Gauge invariance requires invariance of the action under the local group of transformations obtained by replacing $\chi \to \chi(x)$. This can be achieved by replacing the derivative in (22.5) by the covariant derivative $D_\mu = \partial_\mu + ieA_\mu$. Under a local $U(1)$ transformation defined by Equation 22.6 with a space–time dependent function $\chi(x)$, $A\mu(x)$ transforms as $A_\mu \to A_\mu - \partial_\mu\chi$, a generalization of Equation 22.2.

The invariance of Maxwell's equations allows a formulation of classical electromagnetism in terms of 4-vectors and tensors. The equations can be written in a covariant way by introducing the electromagnetic tensor $F_{\mu\nu}$ as follows:

$$F_{0i} = E_i, \quad F_{ij} = -\epsilon_{ijk}B_k, \tag{22.7}$$

and the 4-current $J^\mu = (\rho, \mathbf{J})$ made of charge density and current. In terms of these geometric objects, the four Maxwell equations reduce to

$$\partial_\lambda F_{\mu\nu} + \partial_\mu F_{\nu\lambda} + \partial_\nu F_{\lambda\mu} = 0, \tag{22.8}$$

$$\partial_\mu F_{\mu\nu} = J_\nu. \tag{22.9}$$

The conservation of the current $\partial_\nu J^\nu = 0$ follows from the antisymmetry of $F_{\mu\nu}$. The first equation is a Bianchi identity. It can be integrated by introducing a gauge field A_μ, such that $F_{\mu\nu} = \partial_\mu A_\nu - \partial_\nu A_\mu$. It is readily verified that two gauge fields related by the gauge transformation $A_{0\mu} = A_\mu - \partial_\mu\Omega$ give rise to the same electromagnetic tensor field. Maxwell's equations can be derived from the action

$$S(A, J) = \int d^4x[F_{\mu\nu}F^{\mu\nu} + J_\mu A^\mu], \tag{22.10}$$

which coincides with the full action in quantum electrodynamics.

The concepts of gauge fields and covariant derivatives can be interpreted in the terms of differential geometry. In general, the gauge field has a mathematical interpretation as a Lie connection and is used to construct covariant derivatives acting on fields, whose form depends on the representation of the group under which the field transforms. The field tensor $F_{\mu\nu}$ is a curvature 2-form given by the commutator of two covariant derivatives. It is an element of the Lie algebra associated with the gauge group. The gauge connection generates parallel transport of the geometric objects under gauge transformations. The generalization of $U(1)$ to non-Abelian groups such as SU(N) is straightforward: the main modification arises in the definition of the field strength (22.6) that becomes $F_{\mu\nu} = \partial_\mu A_\nu - \partial_\nu A_\mu + [A_\mu, A_\nu]$.

General relativity can be also interpreted as a gauge theory, where gauge invariance is invariance under diffeomorphisms (local smooth changes of coordinates) in the space–time manifold. The connection, which generates parallel transport, plays the role of the gauge field. Gauge invariance corresponds to the independence of field equations from the choice of the local frame. The spin connection plays the role of the gauge field.

The gauge invariance allows fixing some conditions on the gauge potentials that will not affect the physical properties. In classical electromagnetism, the gauge-fixing problem is simply the problem of choosing a representative in the class of equivalent potentials, convenient for practical calculations or most suited to the physical nature of a particular problem under consideration. In non-relativistic problems, one of the most popular choices is the Coulomb gauge, $\nabla\mathbf{A}(t, \mathbf{x}) = 0$, whose relativistic counterpart is $\partial_\mu A_\mu(t, \mathbf{x}) = 0$ ($\mu = \{0,1,2,3\}$), called Landau or Lorentz's gauge. The freedom of a gauge condition choice is related to the full gauge invariance of the action. When fictitious gauge fields are generated by analogy with the gauge formalism but there is no dynamics associated to them it can happen that the gauge potentials are fixed by the physics involved and no extra conditions can be imposed. Gauge fields were introduced in condensed matter in the early works of References 2 and 3, but now this question is very popular among many researchers [4–7].

The problem of modified graphene properties has attracted a considerable attention (see References 8–12 for instance) because "pure" graphene has no energy gap in the band structure, and, therefore, the creation of different structures (for example, analogs of transistors) is extremely difficult. However, the situation becomes more promising when various modifications of the specimen are introduced. As an example, we consider the modified graphene, for example, graphene nanoribbon, which has quantized electron energy spectrum due to the limited space in one dimension, which in turn can lead to the formation of an energy gap. Furthermore, it is well known that graphene has a naturally wave-like curved surface due to the instability of the planar structure of its sheets [13,14]. All of the above reasons have stimulated the study of different modifications of curved graphene [15,16].

The long-wave approximation—widely used to describe the properties of electrons in graphene—leads to an analog of the Dirac equation, which in turn makes it easy to produce generalization to the case when the graphene surface is curved. Note that, in this case, the degeneracy in the Dirac points disappears and, therefore, it becomes possible to create various structures with different band gaps. Consideration of the Dirac equation for curved graphene [15] also shows a change in the density of states of electrons, and, therefore, it makes it possible to change the whole set of electrical characteristics of a graphene sample. Apparently, the easiest way to experimentally verify those changes in the density of states is to study the tunneling current [17], for example, through the contact with quantum dots. Reducing the size of the particles leads to the manifestation of a very unusual properties of the material from which it is made. The reason for this are quantum-mechanical effects originated from the spatial limitation of charge carriers movements: carriers' energy becomes discrete in this case. The number of energy levels depends on the size of the potential well, the potential barrier height, and the mass of the charge carrier. An increase in the well size leads to an increase in the number of energy levels. Movement of charge carriers can be restricted in one coordinate (forming quantum films), in two coordinates (quantum wires or strands), or in all three areas (quantum dots). Quantum dots are still a rather "young" object of study, but their use in various fields of science and technology is obviously extremely promising (from the design of new lasers and the generation of new displays to building qubits) [18–21].

22.2   GRAPHENE AND ITS HAMILTONIANS

From the chemical point of view, the main element of any graphite compound is a sheet of graphene, which can be regarded as benzene hexagons whose hydrogen atoms are replaced by carbon atoms in the adjacent cells, hexes. The carbon atoms in graphene form a honeycomb-like structure according to the sp2 hybridization. This structure cannot be regarded as a Bravais lattice, since two adjacent cells are not equivalent from the crystallographic point of view.

Let us consider the structure of graphene with two sublattices A and B (Figure 22.1), where a_1 and a_2 are the basis
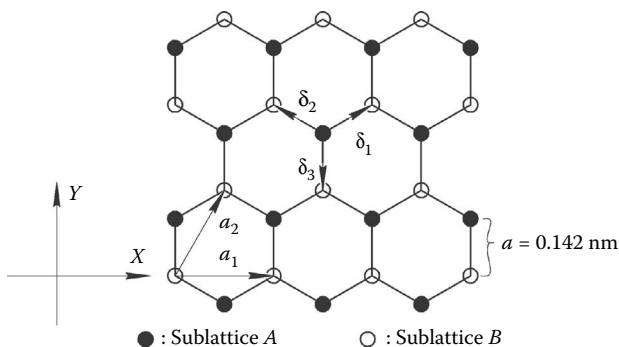
FIGURE 22.1   Crystal lattice of graphene.

vectors; δ_1, δ_2, and δ_3 are the vectors connecting a site of the sublattice A with the nearest neighbor sites of the sublattice B.

This study is required to identify the characteristics of the electronic structure of graphene, the presence of a gap, that will properly take into account the initial conditions of the problem.

Construction of a microscopic model describing the interaction of electrons in graphene has been done within a framework of the Hückel approximation. The Hamiltonian of the electron system was considered in the framework of the Hubbard model for a single-layer graphene. The model takes into account the Coulomb interaction between electrons, which leads to a substantial change in dispersion, and hence in the optical response of the system. Moreover, the account of the electron interaction Hamiltonian leads to a change in the spectrum of elementary excitations of the model:

$$E(\overline{p}) = \frac{\varepsilon(\overline{p})}{2} + \frac{U}{2} \mp \frac{1}{2}\sqrt{\varepsilon^2(\overline{p}) - 2\varepsilon(\overline{p})U(1-2n_0) + U^2},$$

(22.11)

where U is the Coulomb repulsion between electrons trapped at a single site; $\varepsilon(\overline{p})$ is the dispersion, which describes the interaction of electrons and phonons in graphene without the Coulomb repulsion, and n_0 is the average number of the on-site electrons.

Account for impurities in the case of doped graphene was carried out in the framework of the Anderson model, where only the hybridization of electronic subsystems is considered. The latter allowed us to avoid the complexities associated with the lack of a gap in the graphene. The resulting Hamiltonian reads

$$H = H_h + H_{im} + H_{hyb}$$

$$H_h = -\sum_{j\Delta\sigma} t_\Delta \left(a_{j\sigma}^+ b_{j+\Delta\sigma} + b_{j+\Delta\varsigma}^+ a_{j\sigma} \right)$$

$$+ U\sum_j \left(a_{j\sigma}^+ a_{j\sigma} a_{j-\sigma}^+ a_{j-\sigma} + b_{j\sigma}^+ b_{j\sigma} b_{j-\sigma}^+ b_{j-\sigma} \right)$$

$$H_{im} = \sum_j \left(\tilde{\varepsilon} d_{j\sigma}^+ d_{j\sigma} + \tilde{\varepsilon} d_{j-\sigma}^+ d_{j-\sigma} + U_1 d_{j\sigma}^+ d_{j\sigma} d_{j-\sigma}^+ d_{j-\sigma} \right)$$

$$H_{hyb} = V\sum_{j\sigma} \left(a_{j\sigma}^+ d_{j\sigma} + d_{j\sigma}^+ a_{j\sigma} \right),$$

(22.12)

where $a_{j\sigma}^+, a_{j\sigma}, b_{j\sigma}^+, b_{j\sigma}$ are the creation and annihilation operators of electrons with spin σ on two mutually dual carbon sublattices, so that the electrons jump only between the sublattices; t_Δ is the hopping integral between neighboring sites in the sublattices; U is the constant of the Coulomb repulsion of electrons trapped at a single site; $d_{j\sigma}^+, d_{j\sigma}$ are the creation and annihilation operators of the impurity electrons with spin σ; $\tilde{\varepsilon}$ is the impurity level energy; U_1 is the constant of the

Coulomb repulsion of the impurity electrons; V is the overlap integral between the wave functions of the impurity electrons and the π-electrons of carbon, forming the bands. Estimations based on the semi-empirical quantum-chemical method MNDO have shown that typical values for these parameters are $t_\Delta \approx 2$ eV, $U \approx 12$ eV, $U \approx 12$ eV, and $V \approx 2$ eV.

Since the properties of the model described by the Anderson Hamiltonian is quite complicated, we assume that $U \to \infty$, and that all the average values are spatially homogeneous. It should be noted that the approximation $U \to \infty$ is consistent with the quantum-mechanical calculations for graphene-like structures. The spectrum of elementary excitations can be represented by

$$E_\sigma(p) = \frac{1}{2}$$
$$\left[\varepsilon(p) + \varepsilon - n^\sigma + \sqrt{(-\varepsilon(p) + \varepsilon - n^\sigma)^2 + 4(1 - n_\sigma^{im})|V|^2} \right],$$
$$(22.13)$$

where V is the hybridization parameter, $\varepsilon(p)$ is the electron spectrum for graphene, determined from the diagonalized Hamiltonian H_h, n^σ, and n_σ^{im} are the parameters determined by the problem stability conditions.

Let us consider the calculation of the energy eigenvalues for electrons in the crystal lattice of graphene with adsorbed atomic hydrogen [22], which is regarded as an impurity. Such a choice of impurity is motivated by the fact that, in this case, the Coulomb interaction energy of the electrons in the adsorbed atom is zero, as there is only one electron in atomic hydrogen. The hybridization potential $V_{\kappa a}$ in the Anderson Hamiltonian can be estimated from a quantum-chemical approach, as it is defined by the overlap integral of the wave functions of the s-orbital (the hydrogen atom), and p_z-orbitals (carbon atoms in graphene):

$$V = \frac{1}{2}(\beta_H + \beta_C)S_{HC},$$

$$S_{HC} = \int \Psi_{1s}(\mathbf{r})\Psi_{2p_z}(\mathbf{r})d\mathbf{r}, \qquad (22.14)$$

$$\Psi_{1s} = \frac{1}{\sqrt{\pi}}\left(\frac{z}{a_0}\right)^{\frac{3}{2}} e^{-\rho}, \quad \rho = \frac{zr}{a_0}, \quad z(H) = 1;$$

$$\Psi_{2p_z} = \frac{1}{4\sqrt{2\pi}}\left(\frac{z}{a_0}\right)^{\frac{3}{2}} \rho e^{-\frac{\rho}{2}} \cos\theta, \quad \rho = \frac{zr}{a_0}, \quad z(C) = 6;$$

where S_{HC} is the overlap integral of the wave functions, β_H and β_C are the parameters derived from the semi-empirical quantum-chemical method MNDO [23], $\beta_H = -6.99$ eV, $\beta_C = -7.93$ eV, a_0 is the Bohr radius, and z is the atomic charge.

An estimate of the hybridization potential gives a value of $V_{\kappa a} = -1.43$ eV. The energy value is negative, therefore a stable state is formed, which is important for practical applications. To estimate the energy of adsorbed atoms ε_a, the method of images is used, based on the fact that the surface of the conductor is equipotential [24]. As a result, we obtain

$$\tilde{\varepsilon}_a = I + \frac{1}{4\pi\varepsilon_0}\frac{e^2}{4l},$$

where $I = -13.6$ eV is the ionization potential of a hydrogen, e is the elementary charge, ε_0 is the dielectric constant, $l = 1.2$ Å is the distance from the center of the adatom to the plane of its image on the substrate, which is of the order of the atomic radius of the adatom (the length of the adsorption bond). To describe the spectrum of elementary excitations of graphene, we use the classical mathematical technique of Green's functions. The expression of Green's function for the lattice with adsorbed atomic defect can be written as follows:

$$\ll c_{k\sigma} \mid c_{k\sigma}^+ \gg = \frac{i}{2\pi}\frac{(\omega - \varepsilon_a)}{(\omega - \varepsilon_a)(\omega - \varepsilon_k) - |V_{ka}|^2}, \quad (22.15)$$

where $c_k\sigma$, $c_{k\sigma}^+$ are the creation and annihilation Fermi operators, and ω is the energy variable.

The analytical expression for Green's function of the crystal lattice of graphene (22.15) allows us to determine the eigenvalues of the electron energy in the crystal, caused by the adsorption of atomic hydrogen. The eigenvalues of the electron energy of the crystal lattice with attached atomic defects are given by the poles of Green's function:

$$E(k) = \frac{1}{2}\left[\varepsilon_a + \varepsilon_k \pm \sqrt{(\varepsilon_a - \varepsilon_k)^2 + 4|V_{ka}|^2} \right], \quad (22.16)$$

where ε_k is the band structure of the "pure" graphene.

In the case of double-layer graphene, the system has been considered in the framework of tight-binding model for π-electrons using a nearest-neighbor approximation with intraplane and interplane hopping integrals t_0, while the electrostatic potential U was applied between the two layers of graphene. The band structure of bilayer graphene, obtained from this tight binding approximation, gives us the following dispersion relation:

$$E_p^{\pm\pm}(U) = \pm\sqrt{\varepsilon(p)^2 + \frac{t_0^2}{2} + \frac{U^4}{4} \pm \sqrt{\frac{t_0^4}{4} + (t_0^2 + U^2)\varepsilon(p)^2}}.$$
$$(22.17)$$

22.3 MATHEMATICAL RULES

In this work, the transition to curvilinear coordinates has been used. Therefore, it is necessary to do a little mathematical retreat, which will contribute to the understanding of the calculations made in the following paragraphs.

We consider the transition from a coordinate system x^0, x^1, x^2, x^3 to another one $x^{0'}, x^{1'}, x^{2'}, x^{3'}$ by means of the following transformation [25]:

$$x^i = f^i(x^{0'}, x^{1'}, x^{2'}, x^{3'}), \tag{22.18}$$

where f^i are some smooth functions. When the coordinates are transformed according to Equation 22.18, their differentials transforms read [25]

$$dx^i = \frac{\partial x^i}{\partial x'^k} dx'^k. \tag{22.19}$$

It should be noted that here and below, a repeated index implies summation over that index. A contravariant 4-vector is any set of four variables A^i, which are defined through their differentials at the curvilinear transition

$$A^i = \frac{\partial x^i}{\partial x'^k} A'^k. \tag{22.20}$$

Derivatives of some scalar after the coordinate conversion are calculated as follows:

$$\frac{\partial \varphi}{\partial x^i} = \frac{\partial \varphi}{\partial x'^k} \frac{\partial x'^k}{\partial x^i}. \tag{22.21}$$

A covariant 4-vector is any set of four variables A_i, which are converted as derivatives of a scalar using the coordinate transform:

$$A_i = \frac{\partial x'^k}{\partial x^i} A'_k. \tag{22.22}$$

Similarly, the 4-tensors of various ranks are defined. Thus, the contravariant 4-tensor of the second rank A^{ik} is the set of 16 variables that transform as the multiplication of two contravariant vectors, that is, according to the following law:

$$A^{ik} = \frac{\partial x^i}{\partial x'^l} \frac{\partial x^k}{\partial x'^m} A'^{lm}. \tag{22.23}$$

A covariant tensor of the second rank A_{ik} is converted by the law:

$$A_{ik} = \frac{\partial x'^l}{\partial x^i} \frac{\partial x'^m}{\partial x^k} A'_{lm}, \tag{22.24}$$

and the mixed 4-tensor A_k^i by the formula:

$$A_k^i = \frac{\partial x^i}{\partial x'^l} \frac{\partial x'^m}{\partial x^k} A'^l_m. \tag{22.25}$$

These definitions are natural extensions of the definitions of 4-vectors and 4-tensors for the Galilean coordinates, according to which the differentials dx^i are also contravariant vectors, and the derivatives $\partial \phi / \partial x^i$ are the covariant 4-vectors.

The construction rules of 4-tensors by the multiplication or its simplification by other 4-tensors in curvilinear coordinates are the same as for the Galilean coordinates. Definition of the unit 4-tensor δ_k^i also does not change: its components are $\delta_k^i = 0$ for $i \neq k$, and $\delta_k^i = 1$ for $i = k$.

The square of the length element in the curvilinear coordinates is a quadratic form of the differentials dx^i:

$$ds^2 = g_{ik} dx^i dx^k, \tag{22.26}$$

where g_{ik} are the coordinate functions; g_{ik} are symmetric in indices i and k:

$$g_{ik} = g_{ki}, \tag{22.27}$$

Since the multiplication (simplified) g_{ik} on a contravariant tensor $dx^i dx^k$ is a scalar, then g_{ik} is a covariant tensor, which is called the metric tensor. Two tensors A_{ik} and B^{ik} are said to be the inverse of each other, if and only if $A_{ik}B^{kl} = \delta_i^l$. Obviously, the only variables which can determine the relationship between the one and the other are the components of the metric tensors. Such a relationship is given by the following expression

$$A^i = g^{ik}A_k, \quad A_i = g_{ik}A^k. \tag{22.28}$$

In a Galilean coordinates system, this tensor has the components:

$$g_{ik}^{(0)} = g^{ik(0)} = \begin{pmatrix} 1 & 0 & 0 & 0 \\ 0 & -1 & 0 & 0 \\ 0 & 0 & -1 & 0 \\ 0 & 0 & 0 & -1 \end{pmatrix}. \tag{22.29}$$

Now, we consider the covariant differentiation. We define the transformation formula for differentials dA_i. Since a covariant vector is calculated by the following formula:

$$A_i = \frac{\partial x'^k}{\partial x^i} A'_k ,$$

we readily obtain

$$dA_i = \frac{\partial x'^k}{\partial x^i} dA'_k + A'_k d\frac{\partial x'^k}{\partial x^l} = \frac{\partial x'^k}{\partial x^i} dA'_k + A'_k \frac{\partial^2 x'^k}{\partial x^i \partial x^l} dx^l.$$

We now undertake the definition of a tensor which in curvilinear coordinates plays the same role as $\partial A_i / \partial x^k$ in Galilean coordinates. In other words, we must transform $\partial A_i / \partial x^k$ from Galilean to curvilinear coordinates. In curvilinear coordinates, in order to obtain a differential of a vector which behaves like

a vector, it is necessary that the two vectors to be subtracted from each other be located at the same point in space. In other words, we must somehow "translate" one of the vectors (which are separated infinitesimally from each other) to the point where the second is located, after which we determine the difference of the two vectors which we now refer to as one and the same point in space. The operation of translation itself must be defined so that in Galilean coordinates the difference shall coincide with the ordinary differential dA_i. The difference in the components of the two vectors after translating one of them to the point where the other is located will not coincide with their difference before the translation (i.e., with the differential dA_i) [25]. Therefore, to compare two infinitesimally separated vectors we must subject one of them to a parallel translation to the point where the second is located. Let us consider an arbitrary contravariant vector; if its value at the point x^i is A^i, then at the neighboring point $x^i + dx^i$ is equal to $A^i + dA^i$. We subject the vector A^i to an infinitesimal parallel displacement to the point $x^i + dx^i$. We denote the change in the vector which results from this by δA^i. Then, the difference DA^i between the two vectors which are now located at the same point is

$$DA^i = dA^i - \delta A^i, \tag{22.30}$$

$$\delta A^i = -\Gamma^i_{kl} A^k dx^l, \tag{22.31}$$

where Γ^i_{kl} are some functions of coordinates, whose form depends on the choice of the coordinate system. In a Galilean coordinate system all of Γ^i_{kl} are equal to zero.

From this, it is already clear that the quantities Γ^i_{kl} do not form a tensor, since a tensor which is equal to zero in one coordinate system is equal to zero in every other one. In a curvilinear space, it is of course impossible to make all Γ^i_{kl} vanish over all of space. But we can choose a coordinate system for which Γ^i_{kl} become zero over a given infinitesimal region (see the end of this section). The quantities Γ^i_{kl} are called Christoffel symbols. In addition to the quantities Γ^i_{kl}, we shall later also use quantities $\Gamma_{i,kl}$, defined as follows:

$$\Gamma_{i,kl} = g_{im} \Gamma^m_{kl}. \tag{22.32}$$

Conversely,

$$\Gamma^i_{kl} = g^{im} \Gamma_{m,kl}. \tag{22.33}$$

It is also easy to relate the changes in the components of a covariant vector under a parallel displacement to the Christoffel symbols. To do this, we note that under a parallel displacement, a scalar is unchanged. In particular, the scalar product of two vectors does not change under a parallel displacement. Let A_i and B^i are some covariant and contravariant vectors. Then from $\delta(A_i B^i) = 0$, we have

$$B^i \delta A_i = -A_i \delta B^i = \Gamma^i_{kl} B^k A_i dx^1.$$

Hence, in view of the arbitrariness of B^i, we obtain that

$$\delta A_i = \Gamma^k_{il} A_k dx^l, \tag{22.34}$$

which determines the change of the covariant vector.

Substituting (22.31) and $dA^i = (\partial x'^k / \partial x^i) x^l$ in formula (22.32), we obtain

$$DA^i = \left(\frac{\partial A^i}{\partial x^l} + \Gamma^i_{kl} A^k \right) dx^l. \tag{22.35}$$

Similarly, we find for the covariant vector

$$DA_i = \left(\frac{\partial A_i}{\partial x^l} - \Gamma^k_{il} A_k \right) dx^l. \tag{22.36}$$

Tensors defined by the following formulas (22.35) and (22.36) are called covariant derivatives of the vectors A^i and A_i. We will denote them by $A^i_{;k}$ and $A_{i;k}$. Thus,

$$DA^i = A^i_{;l} dx^1, \quad DA_i = A_{i;l} dx^l, \tag{22.37}$$

while the covariant derivatives themselves are

$$A^i_{;l} = \frac{\partial A^i}{\partial x^l} + \Gamma^i_{kl} A^k, \tag{22.38}$$

$$A_{i;l} = \frac{\partial A_i}{\partial x^l} - \Gamma^k_{il} A_k. \tag{22.39}$$

In a Galilean coordinate system, all coefficients $\Gamma^i_{kl} = 0$ and covariant derivatives are reduced to ordinary differentiation.

It is also easy to calculate the covariant derivative of a tensor. To do this, we must determine the change in the tensor under an infinitesimal parallel displacement. For example, let us consider any contravariant tensor, expressible as a product of two contravariant vectors $A^i B^k$. Under parallel displacement,

$$\delta(A^i B^k) = A^i \delta B^k + B^k \delta A^i = -A^i \Gamma^k_{lm} B^l dx^m - B^k \Gamma^i_{lm} A^l dx^m.$$

By virtue of the linearity of this transformation we must also have, for an arbitrary tensor A^{ik},

$$\delta A^{ik} = -(A^{im} \Gamma^k_{ml} + A^{mk} \Gamma^i_{ml}) dx^l. \tag{22.40}$$

Hence, we find covariant derivative of the tensor in the following form:

$$A^{ik}_{;l} = \frac{\partial A^{ik}}{\partial x^l} + \Gamma^i_{ml} A^{mk} + \Gamma^k_{ml} A^{im}. \tag{22.41}$$

Quite similarly, we obtain the covariant derivative of the mixed tensor A_k^i and the covariant tensor A_{ik} in the form

$$A_{k;l}^i = \frac{\partial A_k^i}{\partial x^l} - \Gamma_{kl}^m A_m^i + \Gamma_{ml}^i A_k^m$$

$$A_{ik;l} = \frac{\partial A_{ik}}{\partial x^l} - \Gamma_{il}^m A_{mk} - \Gamma_{kl}^m A_{im}.$$

(22.42)

One can similarly determine the covariant derivative of a tensor of arbitrary rank. In doing so, one finds the following rule of covariant differentiation: to obtain the covariant derivative of the tensor A::: with respect to x^l, we add to the ordinary derivative $\partial A:::/\partial x^l$ for each covariant index $i(A{:}i{:})$ a term $-\Gamma_{il}^k$. One can easily verify that the covariant derivative of a product is found by the same rule as for ordinary differentiation of products. In doing so, we must consider the covariant derivative of a scalar as an ordinary derivative, that is, as the covariant vector $\phi_k = \partial\phi/\partial x$, in accordance with the fact that for a scalar $\delta\phi = 0$, and therefore $D\phi = d\phi$. For example, the covariant derivative of the product $A_i B_k$ is given by

$$(A_i B_k)_{;l} = A_{i;l} B_k + A_i B_{k;l}.$$

If in a covariant derivative we raise the index signifying the differentiation, we obtain the so-called contravariant derivatives:

$$A_i^{;k} = g^{kl} A_{i;l}, \quad A^{i;k} = g^{kl} A_{;l}^i.$$

Now, we have the formulas for transforming the Christoffel symbols from one coordinate system to another. These formulas can be obtained by comparing the laws of transformation of the two sides of the equations defining the covariant derivatives, and requiring that these laws be the same for both sides. It is straightforward to get [25]

$$\Gamma_{kl}^i = \Gamma_{np}^{\prime m} \frac{\partial x^i}{\partial x^{\prime m}} \frac{\partial x^{\prime n}}{\partial x^k} \frac{\partial x^{\prime p}}{\partial x^l} + \frac{\partial^2 x^{\prime m}}{\partial x^k \partial x^l} \frac{\partial x^i}{\partial x^{\prime m}}. \quad (22.43)$$

It can be seen that values Γ_{kl}^i behave like a tensor only under linear transformations of the coordinates (when the second term disappears in the expression (22.43)). The relationship between the Christoffel symbols and the metric tensor, and its first coordinate derivatives can be written in the following form [25]:

$$\Gamma_{\mu\nu}^\alpha = \frac{1}{2} g^{\alpha\beta} \left(\frac{\partial g_{\mu\beta}}{\partial x^\nu} + \frac{\partial g_{\beta\nu}}{\partial x^\mu} - \frac{\partial g_{\mu\nu}}{\partial x^\beta} \right). \quad (22.44)$$

At this point, we turn back to the main goal of our study. The Dirac equation in a carbon nanosystem (CNS), taking into account the curvature of the surface, can be obtained as follows. We introduce a set of orthogonal vectors e_α on the manifold, described by the metric tensor $g_{\mu\nu}$, transforming on the group SO(2): $g_{\mu\nu} = e_\mu^\alpha e_\nu^\beta \delta_{\alpha\beta}$, where e_μ^α is the dyadic coefficients [26], $\alpha, \beta = 1,2$ are the orthonormal indices, and $\mu, \nu = 1,2$ are the coordinate indices. Dyads can be selected with certain gauge freedom, resulting in the emergence of a SO(2)-field ω_μ, which is a spin connection. It should be subjected to a condition analogous to the metric tensor without torsion:

$$D_\mu e_\nu^\alpha := \partial_\mu e_\nu^\alpha - \Gamma_{\mu\nu}^\lambda e_\lambda^\alpha + (\omega_\mu)_\beta^\alpha e_\nu^\beta = 0$$

(elongated derivative of the expression, which has metric and spin indices can be formally written in the following form: $D_\mu = \partial_\mu + \Gamma_\mu + \omega_\mu$), then the spin connection can be defined as

$$(\omega_\mu)^{\alpha\beta} = e_\nu^\alpha D_\mu e^{\beta\nu}.$$

Thus, the Dirac equation, taking into account the curvature of the surface, takes the form:

$$i\gamma^\alpha e_\alpha^\mu (\nabla_\mu - i a_\mu^k - i W_\mu)\psi^k = E\psi^k,$$

where $a_\mu^k, k = K, K_-$ are the Dirac points, W_μ are the gauge fields (defect fields), γ^α are the SU(2)-matrices (special unitary matrices of the second order) 2×2, which can be selected as $\gamma_i = -i\sigma_i$, and $\nabla_\mu = \partial_\mu + \Omega_\mu$, where $\Omega_\mu = (1/8)\omega_\mu^{\alpha\beta}[\gamma_\alpha, \gamma_\beta]$.

22.4 BASIC EQUATIONS AND SPECTRUM OF ELECTRONS

We consider a graphene nanoribbon, which is curved along the toroidal and the helical surfaces, as represented in Figure 22.2. Properties of electrons in graphene nanoribbons in the long-wave approximation and in the vicinity of the Dirac points will be described on the basis of the Dirac equation generalized for the case of a curved space–time [1]:

$$\gamma^\mu (\partial_\mu - \Omega_\mu)\Psi = 0, \quad (22.45)$$

where ∂_μ is the partial derivative with respect to coordinate μ, Ω_μ is the component of the spin connection, $\Psi = (\phi/\varphi)$ is the wave function (column vector) consisting of wave functions describing the electrons from different sublattices near the Dirac point.

As is well known [1,27], if we are given the metric tensor

$$ds^2 = g_{\alpha\beta} dx^\alpha dx^\alpha$$

$$g_{\alpha\beta} g^{\beta\gamma} = \delta_\alpha^\gamma, \quad (22.46)$$

(δ_α^γ—delta is the Kronecker symbol) then we can define the field frames (tetrads):

$$g_{\alpha\beta} = e_\alpha^a e_\beta^b \eta_{ab}$$

$$g^{\alpha\beta} = e_a^\alpha e_b^\beta \eta^{ab} \quad (22.47)$$

$$\eta_{ab} \eta^{bc} = \delta_a^c,$$
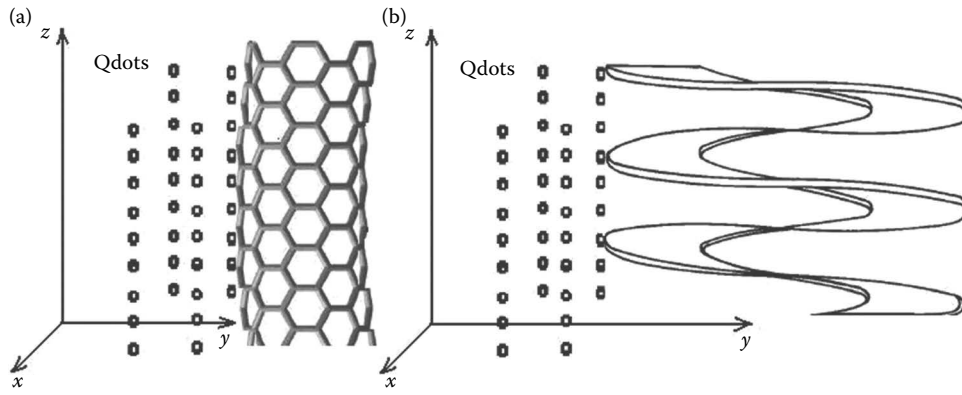
FIGURE 22.2 Geometry of a problem: (a) toroidal nanoribbon, (b) helical nanoribbon. (Adapted from M.B. Belonenko et al. *J. Nanotechnol.* **2011**, ID 161849, 2011.)

where for the two-dimensional curved surfaces, we have $\eta_{ab} = \text{diag}(1, -1, -1)$. Then

$$\Omega_\mu = \frac{1}{4}\gamma_a\gamma_b e^a_\lambda g^{\lambda\sigma}(\partial_\mu e^b_\sigma - \Gamma^\lambda_{\mu\sigma}e^b_\lambda)$$

$$\Gamma^\lambda_{\mu\sigma} = \frac{1}{2}g^{\lambda\nu}(g_{\sigma\nu,\mu} + g_{\nu\mu,\sigma} - g_{\mu\sigma,\nu})$$ (22.48)

$$\gamma^\mu = e^\mu_a\gamma_a.$$

Using the torus and the helical parameterization

$$x = (R + r\cos x_1)\cos x_2$$
$$y = (R + r\cos x_1)\sin x_2$$ (22.49)
$$z = r\sin x_1,$$

$$\begin{cases} x = x_1\cos x_2 \\ y = x_1\sin x_2 \\ z = h\cdot x_2 \end{cases}$$ (22.50)

we find that the metrics on the torus surface and the helicoid are given by

$$ds^2 = dx_0{}^2 - r^2dx_1{}^2 - (R + r\cos x_1)^2 dx_2{}^2,$$ (22.51)

$$ds^2 = dx_0{}^2 - dx_1{}^2 - (h^2 + x_1{}^2)dx_2{}^2.$$ (22.52)

Note that all the Christoffel symbols are equal to zero, except Γ^2_{12} and Γ^1_{22}. For the torus, we have $\Omega_0 = 0$; $\Omega_1 = 0$; $\Omega_2 = (1/2)\gamma_1\gamma_2 f'/r$ ($f = R + r\cos x_1$; $f' = \partial f/\partial x_1$), while in the case of the helicoid $\Omega_0 = 0$; $\Omega_1 = 0$;

$$\Omega_2 = \frac{1}{2}\gamma_1\gamma_2\frac{x_1}{(h^2 + x_1{}^2)^{1/2}}.$$

Choosing $\gamma_0 = \sigma_3$; $\gamma_1 = -i\sigma_2$; $\gamma_2 = -i\sigma_1$, where σ are the Pauli matrices, we obtain the following system of equations:

$$\begin{cases} V_F^{-1}\partial_t\varphi = -\frac{1}{r^2}\partial_{x_1}\Psi - \frac{i}{f^2}\partial_{x_2}\Psi + \frac{f'}{2f^2 r}\Psi \\ V_F^{-1}\partial_t\varphi = -\frac{1}{r^2}\partial_{x_1}\varphi + \frac{i}{f^2}\partial_{x_2}\varphi + \frac{f'}{2f^2 r}\varphi \end{cases},$$ (22.53)

$$\begin{cases} V_F^{-1}\partial_t\varphi + \partial_{x_1}\Psi + \frac{i}{h^2 + x_1{}^2}\partial_{x_2}\Psi - \frac{x_1}{2(h^2 + x_1{}^2)^{3/2}}\Psi = 0 \\ -V_F^{-1}\partial_t\Psi - \partial_{x_1}\varphi + \frac{i}{h^2 + x_1{}^2}\partial_{x_2}\varphi - \frac{x_1}{2(h^2 + x_1{}^2)^{3/2}}\varphi = 0 \end{cases}.$$ (22.54)

Here, V_F is the Fermi velocity for planar graphene, $\partial_0 = V_F^{-1}\partial_t$. Note that since the metrics (22.51) and (22.52) admit two Killing vectors corresponding to the translations along x_0, x_2, the solutions (22.53) and (22.54) can be found in the form $\begin{pmatrix}\varphi \\ \Psi\end{pmatrix} \to \begin{pmatrix}\varphi(x_1) \\ \Psi(x_1)\end{pmatrix}e^{iEt - ikx_2}$, which finally gives

$$\Psi'' = \left(-\frac{E^2 r^4}{V_f^2} + \frac{k_n{}^2 r^4}{f^4}\right)\Psi + \frac{rf'}{2f^2}\Psi'$$

$$+ \left(\frac{2k_n r^2 f'}{f^3} + \frac{rf''}{2f^2} - \frac{rf'^2}{f^3} - \frac{r^2 f'^2}{4f^4}\right)\Psi,$$ (22.55)

$$\Psi'' = \left(-\frac{\varepsilon^2}{V_f^2} + \frac{k^2}{(h^2 + x_1{}^2)^2}\right)\Psi$$

$$+ \left(-\frac{kx_1}{(h^2 + x_1{}^2)^{5/2}} + \frac{x_1{}^2}{4(h^2 + x_1{}^2)^3}\right)\Psi.$$ (22.56)

Note that the wave vector k is found from the boundary conditions at the ends of the nanoribbon. In our particular case, we have chosen the armchair-type ribbon [9], and therefore
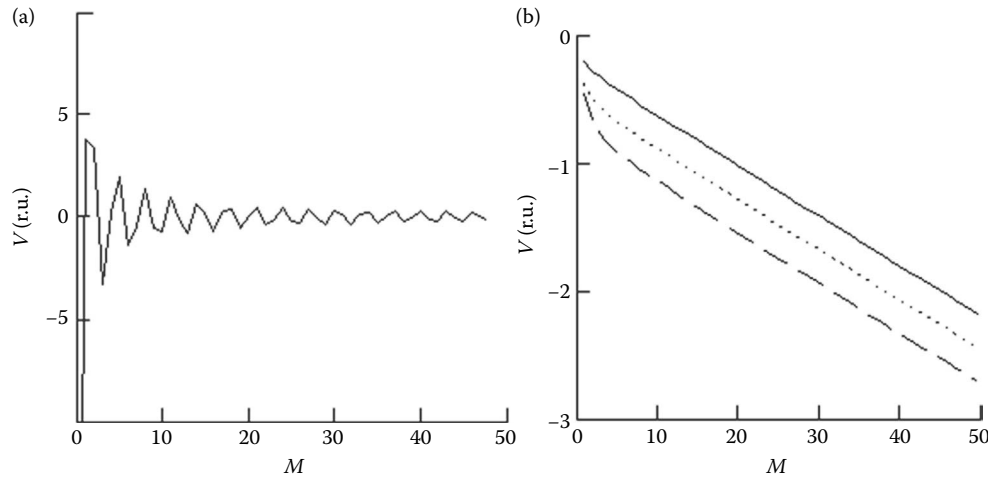
FIGURE 22.3 Dependence of the correction to the energy V caused by the perturbation $\hat{V}$ on atoms number along nanoribbon axis M: (a) for torus ($r/R = 0.1$, $n = 1$); (b) for helicod ($h = 1.5$): (i) $n = 1$—solid line; (ii) $n = 2$—dotted line; (iii) $n = 3$—dashed line. (Adapted from M.B. Belonenko et al. *J. Nanotechnol.* **2011**, ID 161849, 2011.)

$$k_n = \frac{2\pi}{3a_0}\left(\frac{2M+1+n}{2M+1}\right), \qquad (22.57)$$

where a_0 is the distance between the atoms in the carbon lattice, M is the number of atoms along the nanoribbon axis, and n is the quantum number. We can consider Equations 22.55 and 22.56 as Schrödinger equations with perturbation

$$\hat{V}_{\text{Torus}} = \left[\left(\frac{2k_n r^2 f'}{f^3} + \frac{rf''}{2f^2} - \frac{rf'^2}{f^3} - \frac{r^2 f'^2}{4f^4}\right) + \frac{rf'}{2f^2}\partial_x\right],$$

$$\hat{V}_{\text{Helicoid}} = \left(-\frac{kx_1}{(h^2+x_1^2)^{5/2}} + \frac{x_1^2}{4(h^2+x_1^2)^3}\right).$$

In this particular case, the spectrum of perturbation reads

$$E = \pm\sqrt{k_n^2 + k_y^2}. \qquad (22.58)$$

Expanding the functions in the denominator as a Taylor series up to the second order, we calculate the first perturbation correction term to the spectrum, $\hat{V}_{\text{Torus}}$ and $\hat{V}_{\text{Helicoid}}$, as follows

$$E_1 = \int \Psi^*\hat{V}\Psi dx, \quad \Psi_n = A\cdot\text{Sin}(k_n x_1).$$

The integration is performed from 0 to $L = (3M + 1)a_0$ and the corrections are as follows:

$$E_1 = \frac{2}{L}\left\{-\frac{r^2}{4R^2}\text{Sin}(L) + \frac{r^2}{8R^2}\left(1-\frac{1}{k_n}\right)\right.$$

$$\left.\frac{\text{Sin}(2k_n-1)L}{(2k_n-1)} + \frac{r^2}{8R^2}\left(1+\frac{1}{k_n}\right)\frac{\text{Sin}(2k_n+1)L}{(2k_n+1)}\right\}, \qquad (22.59)$$

$$E_1 = \frac{2}{L}\left\{\begin{array}{l}\left(-\frac{kL^2}{4h^5} + \frac{k}{4h^5 k_n^2} + \frac{h^{-2/3}L^3}{24}\right) \\[2mm] + \text{Sin}(2k_n L)\left(\frac{kL}{4h^5 k_n} + h^{-2/3}\left(\frac{1}{32k_n^3} - \frac{L^2}{16k_n}\right)\right) \\[2mm] + \text{Cos}(2k_n L)\left(\frac{-k}{4h^5 k_n^4} + \frac{h^{-2/3}L}{16k_n^2}\right)\end{array}\right\}. \qquad (22.60)$$

The dependence of the perturbations on the atom numbers along the nanoribbons M is presented in Figure 22.3.

The dependence shown in Figure 22.3a is rather complex, which is associated with the quantization of the electron spectrum in graphene nanoribbons in relation with Equation 22.57. It should be noted that the dependence of the energy gap in carbon nanotubes of zigzag type is pretty similar, which also arises from the quantization of the electron spectrum in the direction along the circumference of the nanotube. The calculations show (Figure 22.3a) that the value of the helicoids parameterization h influences most strongly the correction to the energy (as well as its sign). The dependence of the energy correction on the ratio r/R is demonstrated in Figure 22.3.

As expected, the dependence shown in Figure 22.4 shows that with increasing curvature of the graphene nanoribbon (i.e., with increasing ratio r/R), the absolute value of the correction to the energy of the electrons increases [28].

22.5 TUNNELING CHARACTERISTICS

The Hamiltonian of the system of electrons can be written in the following form:

$$H = \sum_p \text{E}_p^A a_p^+ a_p + \sum_q E_q^B b_q^+ b_q + \sum_{pq} T_{pq}(a_p^+ b_q + b_q^+ a_q), \qquad (22.61)$$
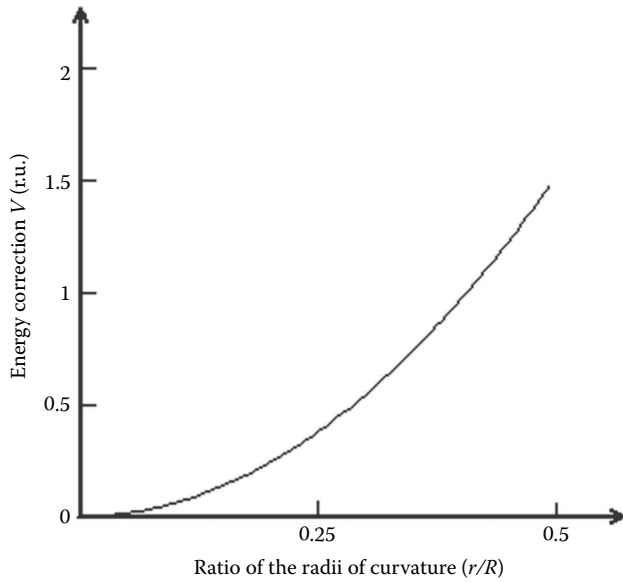
FIGURE 22.4 Dependence of the energy correction V, caused by the perturbation $\hat{V}$, on the ratio of the radii of curvature r/R ($M = 20$, $n = 1$). (Reprinted from *Sol. State Commun.*, **151**, M.B. Belonenko, N.G. et al., 1147, Copyright 2011, with permission from Elsevier.)

where $a_p^+; a_p$ are the electron creation and annihilation operators with momentum p in the carbon nanoribbons; E_p^A is the electron spectrum of the carbon nanoribbons (22.58) while taking into account Equations 22.59 and 22.60; T_{pq} is the matrix element of the tunneling operator between p and q states; $b_q^+; b_q$ are the electron creation and annihilation operators with momentum q in a substance which is in contact with a carbon nanoribbon; E_p^B is the electron spectrum of another substance. It should be noted that p and q are multi-indices in formula (22.61). Hence, for graphene nanoribbon (further, we consider an arm-chair nanoribbon only) $p = (p_y, n)$, $n = 0,1,…,M − 1$. Multi-index q is determined by the substance which is in contact with the carbon nanoribbon, and, for example, for quantum dots $q = (p_x, p_y, p_z)$, whereas for graphene $q = (p_x, p_y)$. A consideration of the external electric field $\vec{E}$ (and choosing $\vec{E} = −(1/c)(\partial \vec{A}/\partial t)$) can be carried out by the canonical transformation $p \rightarrow p − eA/c$.

The tunneling current is considered to be given by

$$J = ie \sum_{pq} (a_p^+ b_q - b_q^+ a_p). \qquad (22.62)$$

With a gauge transformation [29,30], we have

$$a_p \rightarrow S^{-1} a_p S$$

$$S = \exp\left(ieVt \sum_p a_p^+ a_p \right),$$

where V is the applied voltage, and e is the electron charge. Formally, it is possible to reduce a problem of calculation of

the current–voltage characteristics to the calculation of the operator response

$$J_t = ie \sum_{pq} (a_p^+ b_q e^{ieVt} - b_q^+ a_q e^{-ieVt})$$

on the external influence [29,30]

$$H_t = \sum_{pq} T_{pq} \left(a_p^+ b_q e^{ieVt} + b_q^+ a_q e^{-ieVt} \right).$$

The solution was obtained within the framework of the Kubo theory:

$$J = 4\pi e |T|^2 \int_{-\infty}^{\infty} dE \nu_A(E + eV) \nu_B(E) (n_f(E) - n_f(E + eV),$$

$$\nu_A(E) = \sum_p \delta(E - E_p^A); \nu_B(E) = \sum_q \delta(E - E_q^B); \qquad (22.63)$$

where $\delta(x)$ is the Dirac delta function, $\nu_{A(B)}(E)$ is the tunneling density of states; $n_f(E)$ is the equilibrium number of fermions with energy E. The approximation of a "rough" contact is used thereafter, so that $T_{pq} = T$ (this imposes certain restrictions on the contact geometry, i.e., the case discussed below means that nanoribbon should be perpendicular to the contact material surface). For definiteness, we choose the dispersion law for the graphene nanoribbons given by Equations 22.58 through 22.60, and the dispersion law for the quantum dots as the contact material being

$$E_q^A = E_0 - \Delta \cos(p), \qquad (22.64)$$

where E_0 is the electron energy of a quantum well, Δ is the tunneling integral determined by the overlap of electron wave functions in the adjacent wells, and the momentum p is directed along the axis Z.

Equation 22.63 under study has been solved numerically. The current–voltage characteristic of the contact is presented in Figure 22.5.

Figure 22.5 shows the asymmetric behavior of current versus voltage applied to the contact. This is due to both the peculiarities of the electronic structure (density of states) of the metal and graphene nanoribbons, and the processes of carrier recombination in the transition contact, which dominate over the thermal processes when $V > 0$. The resulting dependence may have important practical applications in the study of nanocontacts and the design of tunnel diodes based on graphene nanoribbons. Also, the region with negative differential resistance was observed for some values of V. The presence of such region allows the use of a tunnel diode as a high-speed switch.
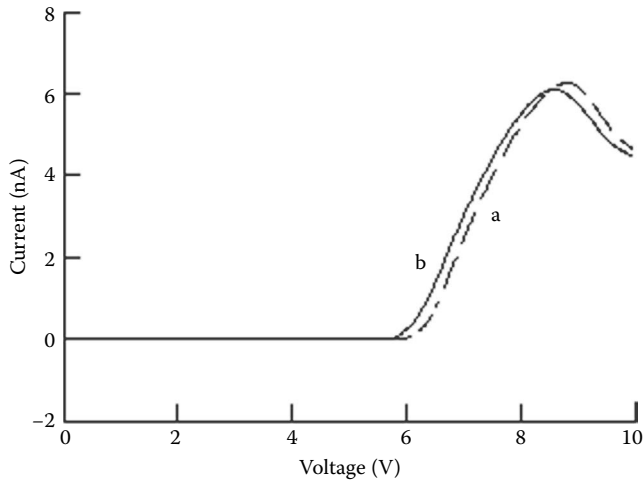
FIGURE 22.5 Current–voltage characteristic of the contact: curved graphene nanoribbon–quantum dots: (a) for torus; (b) for helicoid. (Adapted from M.B. Belonenko et al. *J. Nanotechnol.* **2011**, ID 161849, 2011.)

22.6　FRIEDMANN MODEL

Now, we consider graphene nanoribbons in the Friedmann model of non-stationary universe [25,31]. Properties of electrons in the graphene nanoribbon in the long-wave approximation in the vicinity of the Dirac point will be described on the basis of the generalized Dirac equation for a curved space–time [1] (see Equation 22.45).

For a strained/curved graphene, constantly under the influence of an external variable mechanical force, the effect of this force leads to a periodic change in the distance between the atoms of graphene, which, in turn, leads to a change in the Fermi velocity, vF. Using the analogy with a curved space–time, we can say that this force leads to a periodic change of spatial intervals, which, as is well known, is adequately described in the frame of the Friedmann non-stationary model. The metrics in the Friedmann non-stationary model of the universe has the form:

$$ds^2 = dt^2 - e^{f(t)}(dx^2 + dy^2), \qquad (22.65)$$

where $e^{f(t)} = 1 + a \sin(\omega_0 t)$.

Here, a stands for the relative amplitude of the strain, while ω_0 is the characteristic frequency of oscillatory deformation. There are only four non-zero Christoffel symbols:

$$\Gamma_{11}^0 = \frac{1}{2}e^f f'; \quad \Gamma_{22}^0 = \frac{1}{2}e^f f'; \quad \Gamma_{01}^1 = \frac{f'}{2}; \quad \Gamma_{02}^2 = \frac{f'}{2}.$$

Thus

$$\Omega_0 = 0; \quad \Omega_1 = -\frac{\gamma_0\gamma_1 f' e^{f/2}}{4}; \quad \Omega_2 = -\frac{\gamma_0\gamma_2 f' e^{f/2}}{4}.$$

Let us choose $\gamma_0 = \sigma_3$; $\gamma_1 = -i\sigma_2$; $\gamma_2 = -i\sigma_1$, where σ are the Pauli matrices. Then, we obtain the following system of equations:

$$V_F^{-1}\partial_t\varphi + e^{-f}\partial_{x_1}\psi + \frac{f' e^{-f/2}}{4}\varphi + ie^{-f}\partial_{x_2}\psi - \frac{if' e^{-f/2}}{4}\varphi = 0$$

$$V_F^{-1}\partial_t\psi - e^{-f}\partial_{x_1}\varphi - \frac{f' e^{-f/2}}{4}\psi + ie^{-f}\partial_{x_2}\varphi - \frac{if' e^{-f/2}}{4}\psi = 0$$

$$(22.66)$$

(here, we explicitly introduced the Fermi velocity for the flat graphene via $\partial_0 = V_F^{-1}\partial_t$). It should be noted that the solution of the system (22.66) can be found in the form:

$$\begin{pmatrix} \varphi \\ \psi \end{pmatrix} \to \begin{pmatrix} \varphi \\ \psi \end{pmatrix} e^{ip_x x + ip_y y},$$

then

$$V_F^{-1}\partial_t\varphi + ip_x e^{-f}\psi + \frac{f' e^{-f/2}}{4}\varphi - p_y e^{-f}\psi - \frac{if' e^{-f/2}}{4}\varphi = 0$$

$$V_F^{-1}\partial_t\psi - ip_x e^{-f}\varphi - \frac{f' e^{-f/2}}{4}\psi - p_y e^{-f}\partial_{x_2}\varphi - \frac{if' e^{-f/2}}{4}\psi = 0.$$

$$(22.67)$$

From the Equation 22.67, it is easy to obtain the following equation for the function φ:

$$\varphi_t + g\varphi = 0,$$

$$g = \alpha V_F f' e^{-f/2}, \quad \alpha = \frac{1-i}{4}.$$

Then the substitution: $\varphi \to \varphi \cdot e^{-\int g dt}$ applied in the set of Equation 22.67 yields the non-linear Shrödinger equation with the excitation term (second one), known as the Mathieu equation:

$$\varphi_{tt} + \varphi_t(f' + g^* - g) + |p|^2 e^{-2f}\varphi = 0.$$

Let us choose the trial unexcited function in the form: $\varphi(t) = \varphi_0 e^{i\omega t}$, and besides $f = 0$. In the non-perturbed case, we obtain the spectrum:

$$\omega^2 = |p|^2. \qquad (22.68)$$

Let us calculate the first energy correction, $\hat{V}$:

$$E_1 = \int \Psi^* \hat{V}\Psi dx, \quad \Psi_n = A \cdot \text{Sin}(k_n x_1),$$

$$\hat{V} = (f' + g^* - g)\partial_t.$$
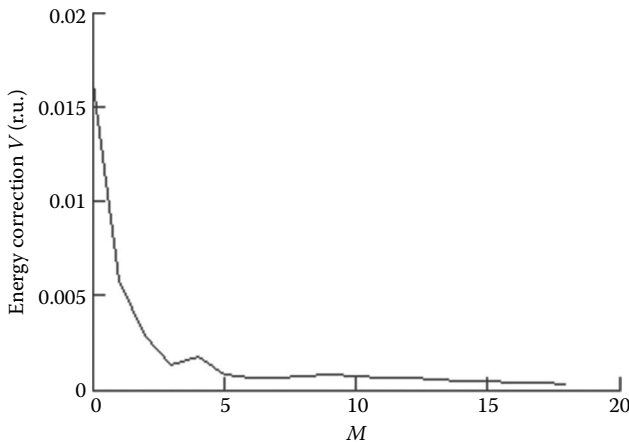
FIGURE 22.6 Dependence of the energy correction V, caused by the perturbation, on the number of atoms M along the axis of the nanoribbon ($n = 1$) in Friedman model.

The integration is done from 0 to $L = (3M + \text{т}1)a_0$ and results in

$$E_1 = \frac{2}{L}\left\{ \frac{k_n \sin(2k_n t)}{4} \cdot \frac{a\omega_0 \cos(\omega_0 t)}{1 + a\sin(\omega_0 t)}\left(1 + \frac{1}{\sqrt{1 + a\sin(\omega_0 t)}}\right)\right\}. \tag{22.69}$$

The dependence of the energy correction on the atom numbers M is demonstrated in Figure 22.6.

This dependence has a step-like form, which is associated with the quantization of the electron spectrum in graphene nanoribbons according to Equation 22.69. Note that this is similar to the dependence of the energy gap in zigzag-type carbon nanotubes [32], which also arises from the quantization of the electron spectrum in the direction along the circumference of the nanotube.

Furthermore, it is worth characterizing the dependence of V on the parameters ω_0 and n. This dependence is shown in
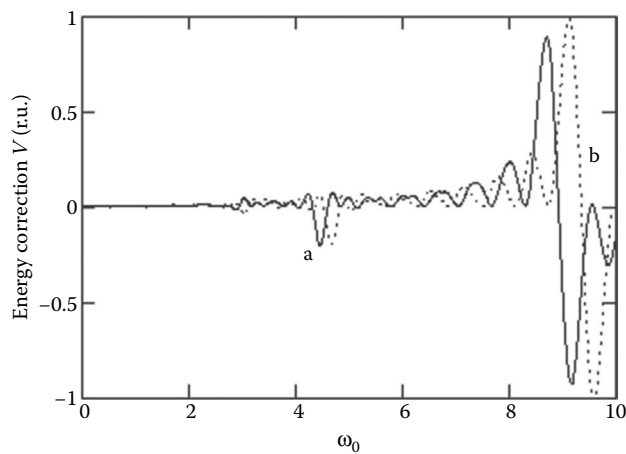
FIGURE 22.7 Dependence of the energy correction V, caused by the perturbation, on the parameter ω_0 for $M = 20$. (a) $n = 1$; (b) $n = 3$. (Adapted from A.V. Zhukov et al. *JETP Lett.* **97**, 400, 2013.)

Figure 22.7, and it demonstrates that with the increase of the characteristic frequency ω_0, we observe a periodic change of the correction to the energy of the electrons. With increasing quantum number n, we observe a shift to the right and a remarkable increase in the amplitude [31].

Also, we constructed the current–voltage characteristics of the contact between a curved nanoribbon and a metal. This dependence shows the asymmetric behavior of current versus voltage applied to the contact, as in the case where we do not take into account the Friedmann model.

22.7 CONCLUSION

In this chapter, we first briefly overviewed the formal relation between the quantum field theory, the general relativity, and the condensed matter of graphene-based nanostructures. Proceeding to the more practical applications, we summarized our studies on the tunnel characteristics between a curved/strained graphene and a metal, considering different geometrical configurations of a graphene sheet. As a result, we have demonstrated that the above contacts behave similarly to classical diodes, which may have important practical applications in the study of nanocontacts and the design of tunnel diodes based on graphene nanoribbons. Moreover, applying the non-stationary Friedmann model leads us to the same qualitative conclusion.

ACKNOWLEDGMENTS

REFERENCES

1. M.A.H. Vozmediano, M.I. Katsnelson, F. Guines. Gauge fields in graphene. *Phys. Rep.* **496**, 109, 2010.
2. I. Dzyaloshinskii, G.E. Volovik. On the concept of local invariance in the theory of spin glasses. *J. de Phys.* **39**, 693, 1978.
3. I. Dzyaloshinskii, G.E. Volovik. Poisson brackets in condensed matter. *Ann. Phys.* **125**, 67, 1980.
4. A.A. Pacheco Sanjuan, Z. Wang, H. Pour Imani, M. Vanević, S. Barraza-Lopez. Graphene's morphology and electronic properties from discrete differential geometry. *Phys. Rev. B.* **89**, 121403(R), 2014.
5. F.M.D. Pellegrino, L. Chirolli, Rosario Fazio, V. Giovannetti, Marco Polini. Theory of integer quantum Hall polaritons in graphene. *Phys. Rev. B.* **89**, 165406, 2014.
6. J.V. Sloan, A.A. Pacheco Sanjuan, Z. Wang, C. Horvath, S. Barraza-Lopez. Strain gauge fields for rippled graphene membranes under central mechanical load: An approach beyond first-order continuum elasticity. *Phys. Rev. B.* **87**, 155436, 2013.
7. D.-W. Zhang, C.-J. Shan, F. Mei, M. Yang, R.-Q. Wang, S.-L. Zhu. Valley-dependent gauge fields for ultracold atoms in square optical superlattices. *Phys. Rev. A.* **89**, 015601, 2014.

8. Y. Zhang, J.W. Tan, H.L. Stormer, P. Kim. Experimental observation of the quantum Hall effect and Berry's phase in graphene. *Nature* **438**, 201, 2005.

9. S. Stankovich, D.A. Dikin, G.H.B. Dommett, K.M. Kohlhaas, E.J. Zimney, E.A. Stach, R. D. Piner, S.T. Nguyen, R.S. Ruoff. Graphene-based composite materials. *Nature* **442**, 282, 2006.

10. A. Zhang, Z. Dai, L. Shi, Y. Ping Feng, C. Zhang. Energy gap opening and quenching in graphene under periodic external potentials. *J. Chem. Phys.* **133**, 224705, 2010.

11. J. Dauber, B. Terrés, C. Volk, S. Trellenkamp, C. Stampfer. Reducing disorder in graphene nanoribbons by chemical edge modification. *Appl. Phys. Lett.* **104**, 083105, 2014.

12. S. Dubey, V. Singh, A.K. Bhat, P. Parikh, S. Grover, R. Sensarma, V. Tripathi, K. Sengupta, M.M. Deshmukh. Tunable superlattice in graphene to control the number of Dirac points. *Nano Lett.* **13**, 3990, 2013.

13. A. Cortijo, M.A.H. Vozmediano. Effects of topological defects and local curvature on the electronic properties of planar graphene. *Nucl. Phys. B.* **76**3, 293, 2007.

14. A. Cortijo, M.A.H. Vozmediano. Electronic properties of curved graphene sheets. *EPL.* **77**, 47002, 2007.

15. D.V. Kolesnikov, V.A. Osipov. Electronic structure of negatively curved graphene. *JETP Lett.* **87**, 419, 2008.

16. L. Brey, H.A. Fertig. Electronic states of graphene nanoribbons studied with the Dirac equation. *Phys. Rev. B.* **73**, 235411, 2006.

17. M.B. Belonenko, N.G. Lebedev, N.N. Yanyushkina. Tunneling through the carbon nanotube/graphene interface exposed to a strong oscillating electric field. *J. Nanophotonics.* **4**, 041670, 2010.

18. N. Cobayasi. *Introduction in Nanotechnology.* Moscow: BINOM, 2007.

19. X. Gao, E. Nielsen, R.P. Muller, R.W. Young, A.G. Salinger, N.C. Bishop, M.P. Lilly, M.S. Carroll. QCAD simulation and optimization of semiconductor quantum dots. *J. Appl. Phys.* **114**, 164302, 2013.

20. D. Solenov, S.E. Economou, T.L. Reinecke. Excitation spectrum as a resource for efficient two-qubit entangling gates. *Phys. Rev. B.* **89**, 155404, 2014.

21. A. Ayachi, W. Ben Chouikha, S. Jaziri, R. Bennaceur. Telegraph noise effects on two charge qubits in double quantum dots. *Phys. Rev. A.* **89**, 012330, 2014.

22. M.B. Belonenko, A.S. Popov, N.G. Lebedev, A.V. Pak, A.V. Zhukov. Extremely short optical pulse in a system of nanotubes with adsorbed hydrogen. *Phys. Lett. A.* **375**, 946, 2011.

23. N.F. Stepanov. *Quantum Mechanics and Quantum Chemistry.* Moscow: Mir, 2001.

24. G.A. Mironova. *Condensed Matter. From Structural Units to Living Matter.* Moscow: MGU, 2004.

25. L.D. Landau, E.M. Lifshitz. *The Classical Theory of Fields.* 4th Ed. Oxford: Butterworth-Heinemann, 2000.

26. V.A. Osipov, E.A. Kochetov, M. Pudlak. Electronic structure of carbon nanoparticles. *J. Exp. Theor. Phys.* **96**, 140, 2003.

27. N.D. Birrel, P.C. W. Davies. *Quantum Fields in Curved Space.* Cambridge: Cambridge University Press, 1982.

28. L.S. Levitov, A.V. Shitov. *Green's Functions. Tasks with Answers.* Moscow: Fizmatlit, 2003, 392 p.

29. M.B. Belonenko, N.G. Lebedev, A.V. Zhukov, N.N. Yanyushkina. Electron spectrum and tunneling current of the toroidal and helical graphene nanoribbon-quantum dots contact. *J. Nanotechnol.* **2011**, ID 161849, 2011.

30. M.B. Belonenko, N.G. Lebedev, N.N. Yanyushkina, A.V. Zhukov, M. Paliy. Electronic spectrum and tunneling current in curved graphene nanoribbons. *Sol. State Commun.* **151**, 1147, 2011.

31. A.V. Zhukov, R. Bouffanais, N.N. Konobeeva, M.B. Belonenko. On the electronic spectrum in curved graphene nanoribbons. *JETP Lett.* **97**, 400, 2013.

32. M.S. Dresselhaus, G. Dresselhaus, P. Avouris. *Carbon Nanotubes: Synthesis, Structure, Properties, and Applications.* Berlin: Springer, 2001.